Pathological response and tumor regression grading following neoadjuvant chemo-immunotherapy and chemotherapy in resectable non-small cell lung cancer

ÖZGE KAYA KORKMAZ[1], YAREN SARI ÇATALDAŞ[1], NAZLICAN SALTIK BAREL[1] and MEHMET BÜYÜKEVLI[2]

[1]Department of Pathology, Etlik City Hospital, University of Health Sciences, Ankara, Ankara 06010, Turkey;
[2]Department of Thoracic Surgery, Etlik City Hospital, University of Health Sciences, Ankara, Ankara 06010, Turkey

Received February 20, 2026; Accepted May 1, 2026

DOI: 10.3892/ol.2026.15667

Abstract. Recent neoadjuvant trials in lung cancer have demonstrated meaningful survival advantages, highlighting the need for standardized assessment of pathologic response in resected specimens. Only two systems are currently recommended for evaluating post-treatment response, namely the International Association for the Study of Lung Cancer (IASLC) tumor regression grading system and the immune-related pathologic response criteria (irPRC). The present study aimed to review and apply histopathologic parameters for assessing tumor regression in non-small cell lung carcinoma (NSCLC) specimens resected after neoadjuvant therapy. A total of 30 NSCLC resections obtained after neoadjuvant therapy between 2022 and 2025 were analyzed. Gross and microscopic evaluations were performed according to IASLC recommendations. Residual viable tumor, fibrosis, inflammation and necrosis were semi-quantitatively assessed according to IASLC and irPRC principles. Major pathologic response (mPR) was defined as ≤10% viable tumor and pathologic complete response (pCR) as 0% viable tumor. Associations with demographic features, treatment modalities and survival outcomes were analyzed. Compared with chemotherapy (CT) alone, chemo-immunotherapy (CIT) exhibited a trend toward a deeper pattern of tumor regression, reflected by lower median viable tumor percentages (7.5 vs. 55.0%) and higher mPR rates (62.5 vs. 22.7%), although these differences did not reach statistical significance. pCR occurred in 37.5% of patients treated with CIT and in 13.6% of patients treated with CT. CIT specimens demonstrated more prominent immune-mediated stromal changes, including greater intratumoral inflammation (32.5 vs. 10.0%) and more frequent lymphocytic patterns. Fibrosis strongly correlated with response (P<0.001), whereas necrosis did not. Spread through air spaces positivity was found to be significantly reduced in cases of mPR (P<0.001). Therefore, neoadjuvant CIT may be associated with deeper pathologic regression compared with CT, characterized by increased fibrosis and immune activation. Major pathologic response remains a potential prognostic indicator and integration of IASLC and irPRC criteria, together with tumor microenvironment assessment, may improve the evaluation of treatment response in resectable NSCLC.

Correspondence to: Dr Özge Kaya Korkmaz, Department of Pathology, Etlik City Hospital, University of Health Sciences, 5 Halil Sezai Erkut Caddesi, Varlık Mahallesi, Yenimahalle, Ankara, Ankara 06010, Turkey
E-mail: balzoge4@gmail.com

Key words: non-small cell lung carcinoma, neoadjuvant therapy, chemo-immunotherapy, tumor regression grading, pathological response

Introduction

NSCLC accounts for ~85% of all lung cancer cases and is the leading cause of cancer-related mortality worldwide, with an estimated 2.2 million new cases and 1.8 million deaths annually (1). Neoadjuvant therapy has become an established method for the management of initially unresectable stage IIIA and stage IV non-small cell lung carcinoma (NSCLC) at the time of diagnosis (2,3). It is particularly beneficial for achieving tumor downstaging in cases with single-station N2 lymph node involvement or large tumors associated with arterial or venous invasion. Accumulating evidence has indicated that, particularly with the addition of immunotherapy to conventional chemotherapy (CT) regimens, neoadjuvant treatment improves survival and resectability while also enhancing pathologic response rates (4,5).

To address this need, the International Association for the Study of Lung Cancer (IASLC) has published comprehensive multidisciplinary recommendations for the pathologic evaluation of lung cancer resection specimens following neoadjuvant therapy (5). These guidelines emphasize meticulous identification and sampling of the tumor bed, quantification of residual viable tumor (RVT) and uniform definitions for major pathologic response (mPR), defined as ≤10% RVT and pathologic complete response (pCR), defined as 0% RVT, irrespective of treatment modality.

However, the addition of immunotherapy to conventional CT has highlighted the need to incorporate new regression patterns into tumor regression grading systems. Features such

as proliferative fibrosis, neovascularization, dense lymphocytic infiltrates, foamy macrophages and stromal alterations have led to the development of a quantitative scoring system referred to as the immune-related pathologic response criteria (irPRC) (6).

The density of tumor-infiltrating lymphocytes (TILs) within the tumor microenvironment has emerged as an important parameter following neoadjuvant therapy (7,8) Tumor cells exhibit enhanced glycolytic activity, resulting in increased lactate production and accumulation within the tumor microenvironment, which has been shown to suppress T-cell function and promote immunosuppression. In this context, tumor-derived metabolic alterations, particularly lactate accumulation, have been shown to suppress T-cell function and promote an immunosuppressive microenvironment (9). The irPRC system has been applied across multiple tumor types, including NSCLC, melanoma, urothelial carcinoma and breast cancer, in patients treated with PD-1/PD-L1 inhibitors (6,10-12).

Pivotal clinical trials have further highlighted the importance of standardized pathologic assessment. The phase III CheckMate 816 trial (trial no. NCT02998528) demonstrated that the addition of nivolumab to platinum-doublet chemotherapy significantly increases both mPR and pCR rates compared with chemotherapy alone, while maintaining surgical safety and feasibility (13). Similarly, the Lung Cancer Mutation Consortium 3 (LCMC3) trial (trial no. NCT02927301), which evaluated neoadjuvant atezolizumab monotherapy, reported meaningful pathological responses, including 20% mPR and 7% pCR, supporting the biological activity of single-agent immunotherapy in early-stage NSCLC (14). These results underscore the ability of immunotherapy to induce deeper tumor regression compared with traditional cytotoxic treatment.

The pathologist serves a central role in the quantitative assessment of these responses. Distinguishing viable tumor from therapy-induced stromal changes, defining the boundaries of the tumor bed and assessing the extent of necrosis can present challenges in routine practice. Therefore, the application of standardized criteria is important (15). Tumor bed mapping and the identification of immune-mediated regression features, such as proliferative fibrosis, neovascularization, dense lymphocytic infiltrate and foamy macrophages, are required for accurate interpretation of post-treatment resection specimens (16).

Comparative studies have provided additional insight into histologic patterns associated with different neoadjuvant treatment modalities, with a number of studies having suggested that, compared with CT alone, chemo-immunotherapy (CIT) may be associated with more pronounced fibrotic remodeling, denser TIL infiltration, lower viable tumor burden and a reduced frequency of adverse prognostic features, such as spread through air spaces (STAS) and pleural invasion (4,17-19).

Collectively, the existing literature demonstrates that standardized evaluation integrating both IASLC and irPRC principles is important in accurately quantifying therapeutic effect, predicting clinical outcomes and enabling comparison across neoadjuvant trials. Despite notable progress, real-world studies comparing histologic response patterns between CT and CIT remain limited, particularly regarding the association between fibrosis, inflammation, necrosis, STAS and survival outcomes. Therefore, the present study aimed to address this gap by systematically evaluating pathologic response and regression features in NSCLC resection specimens following neoadjuvant therapy using both IASLC and irPRC frameworks. Proportional assessment of residual tumor, fibrosis, inflammation, necrosis and the tumor bed may thus reveal differences in treatment response between CT and CIT protocols.

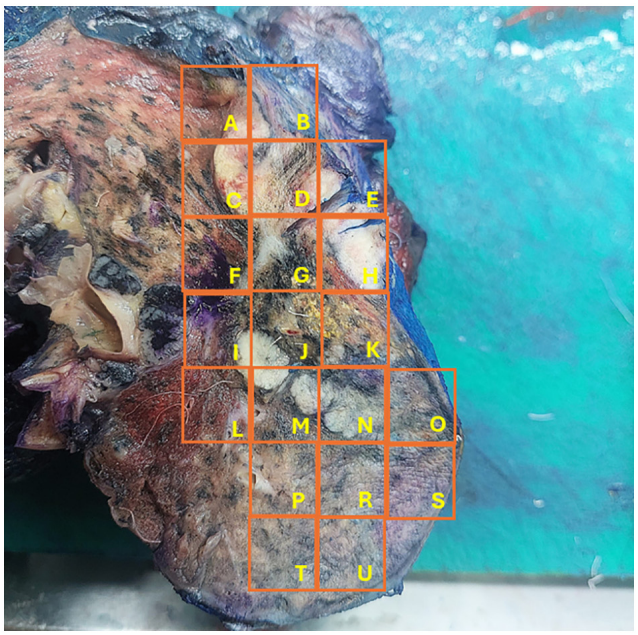

Figure 1. Gross assessment and mapping of the tumor bed following neoadjuvant therapy. The specimen was systematically sectioned and subdivided into grid areas (A-U) for representative sampling according to International Association for the Study of Lung Cancer recommendations.

Materials and methods

Patient selection. The present retrospective study included resected lung cancer specimens from patients who underwent neoadjuvant CT or CIT at the Department of Pathology, Etlik City Hospital, Ankara, Türkiye, between November 2022 and July 2025. Clinical data were obtained from medical records, including age, sex, smoking history, treatment regimen, clinical stage, radiologic findings and follow-up information.

Inclusion criteria were as follows: i) histologically confirmed non-small cell lung cancer (NSCLC); ii) receipt of neoadjuvant CT or CIT followed by surgical resection; and iii) availability of adequate pathological material for evaluation. Exclusion criteria included: i) incomplete clinical or follow-up data; ii) insufficient tumor tissue for histopathological assessment; and iii) prior history of other malignancies or previous lung cancer treatment.

The present study was conducted in accordance with the Declaration of Helsinki and was approved by the Ethics Committee of Etlik City Hospital (approval no. AEŞH-BADEK2-2025-285). The requirement for informed consent was waived due to the retrospective nature of the study.

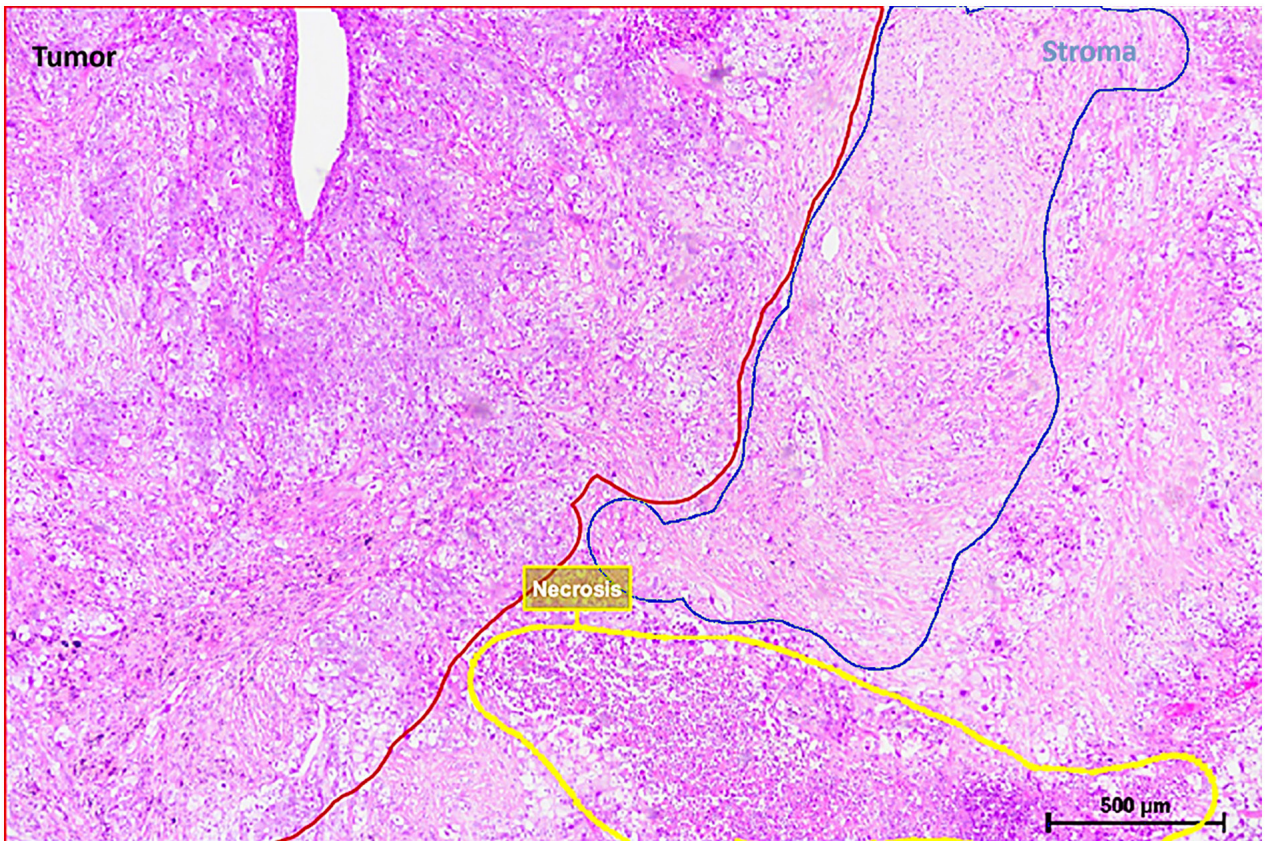

Figure 2. Representative histologic image demonstrating manual annotation of viable tumor (red), stromal component (blue) and necrotic areas (yellow) using QuPath software for quantitative assessment (scale bar, 500 μm).

Pathologic examination. All resection specimens were grossly examined in accordance with IASLC recommendations, with particular attention paid to accurate identification and mapping of the tumor bed (5). Fibrotic and necrotic areas within the tumor bed were extensively sampled, and the entire tumor bed was comprehensively submitted for histopathological evaluation to ensure adequate representation of treatment-induced changes. As shown in Fig. 1, each specimen was systematically sectioned and subdivided into grid areas to enable precise mapping and comprehensive assessment of the tumor bed (Fig. 1). Representative sections were obtained from the entire tumor bed, including areas of fibrosis, necrosis, and any residual viable tumor. All nodal stations were systematically evaluated to assess metastatic involvement. Lymph nodes from each station were dissected and entirely submitted for histological evaluation when feasible.

Surgical specimens were fixed in 10% neutral buffered formalin (Sigma-Aldrich; Merck KGaA) at room temperature for 24-48 h. Following fixation, tissues were routinely processed using an automated tissue processor and embedded in paraffin. Paraffin blocks were sectioned at a thickness of 4 μm using a rotary microtome and mounted on glass slides Histopathological assessment focused on quantifying the percentage of RVT and assigning tumor regression grade according to established criteria (5,6). The pattern and extent of fibrosis, the presence and degree of coagulative necrosis and the distribution of inflammatory infiltrates, including stromal and intratumoral TILs, were documented. Briefly, sections were deparaffinized in xylene and rehydrated through graded ethanol solutions. Hematoxylin staining (Harris hematoxylin; Sigma-Aldrich; Merck KGaA) was performed for 5-7 min at room temperature, followed by rinsing in running tap water and differentiation. Slides were counterstained with eosin Y solution (Sigma-Aldrich; Merck KGaA) for 1-2 min at room temperature, dehydrated through graded alcohols, cleared in xylene, and coverslipped using a mounting medium. All stained slides were examined using a light microscope. Histopathological evaluation was performed independently by experienced pathologists. Whole-slide images were reviewed using QuPath (version 0.6.0) (20). Tumor, necrotic and stromal regions were manually delineated using annotation tools and area measurements were extracted to calculate the relative proportions of each tissue component (Fig. 2). Additional regression-associated features such as foamy macrophages, cholesterol clefts and hemosiderin deposition were evaluated. Adverse morphologic parameters, including STAS and pleural invasion, were recorded when present. Lymph nodes were also examined for residual metastatic tumor. All histopathologic evaluations were performed jointly by three pathologists. Cases were reviewed in a consensus-based manner and any discrepancies in the assessment of histologic parameters were resolved through joint re-evaluation and agreement. Although formal interobserver variability was not quantified, a standardized evaluation approach based on IASLC recommendations was applied to ensure consistency (5). Digital quantification using QuPath was applied to obtain objective measurements of tumor, stromal and necrotic components. Although manual annotation was required for region selection,

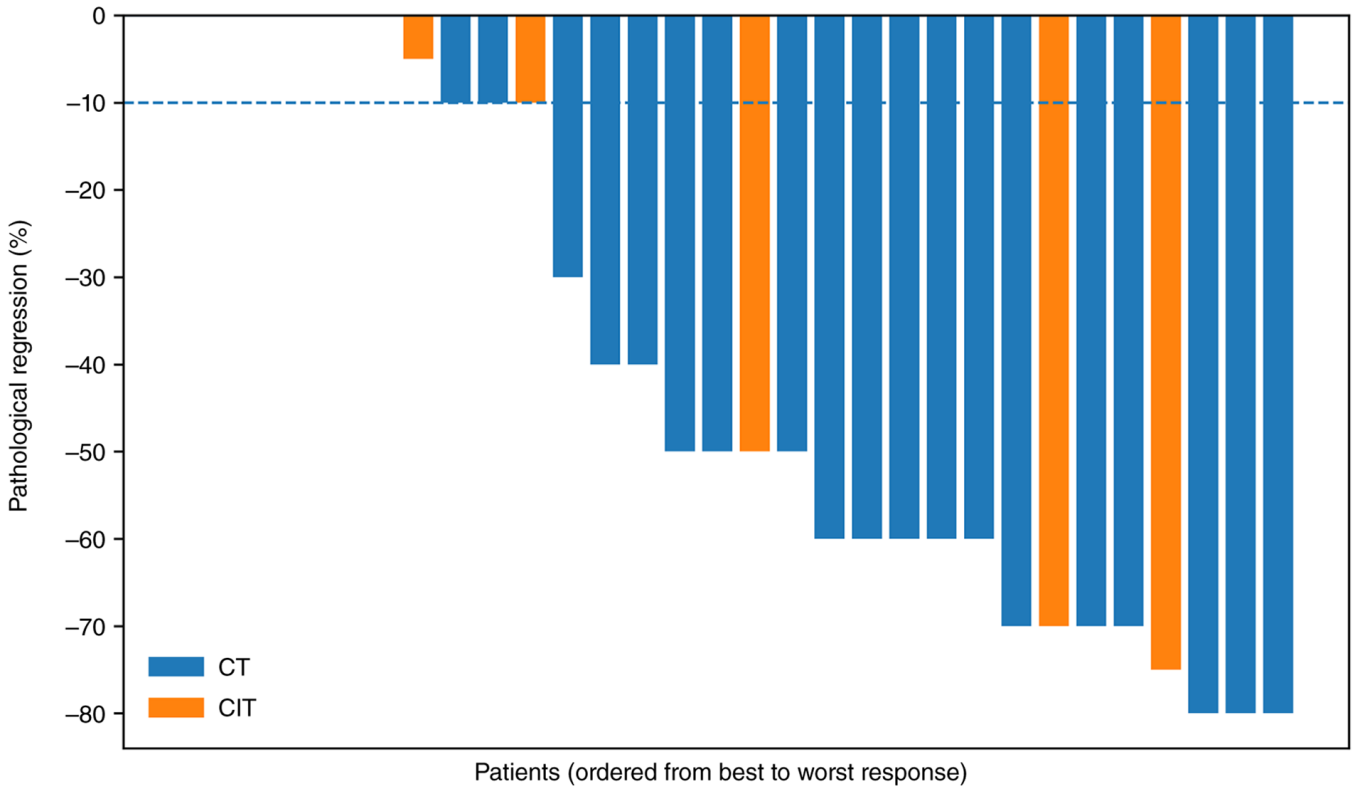

Figure 3. Waterfall plot to visualize the depth of pathologic response for each patient. CT, chemotherapy; CIT, chemo-immunotherapy.

the use of a standardized digital analysis platform helped reduce observer-dependent variability.

Criteria for pathologic response. Pathologic response was assessed in accordance with established neoadjuvant therapy criteria (5,6) pCR represented the complete absence of viable tumor cells in the resected lung specimen and regional lymph nodes and mPR was defined by an RVT fraction of ≤10%, indicative of notable treatment effect. Specimens with >10% viable tumor were classified as non-mPR, reflecting limited pathologic regression.

Statistical analysis. Statistical analyses and data visualization were performed using the Python programming language (Version 3.13.7; Python Software Foundation). The distribution characteristics of continuous variables were assessed using the Shapiro-Wilk and Kolmogorov-Smirnov test. For data that did not follow a normal distribution and for variables with limited sample size, descriptive statistics are reported as the median [interquartile range (IQR): 25-75th percentile], while categorical variables are presented as frequencies (n) and percentages (%). The nonparametric Mann-Whitney U test was used to compare continuous variables between two independent groups. For categorical variables, Fisher's exact tests and χ^2 tests were preferred due to the small sample size and low expected cell frequencies. Spearman's rank analysis was applied to examine correlation between variables. $P<0.05$ was considered to indicate a statistically significant difference for all analyses. Given that the dataset lacked exact dates of mortality and recurrence, survival analysis was conducted using a pseudo-overall survival (pseudo-OS) approach based on the time from diagnosis to the last follow-up date.

Results

Patient characteristics and clinicopathological data. A total of 30 patients diagnosed with resectable NSCLC who received neoadjuvant therapy were included in the present study. The median age was 65.0 years (IQR: 59.2-68.5) and the majority of patients were male (93.3%). Patients were divided into two cohorts according to the treatment regimen administered. The CT cohort consisted of 22 patients (73.3%) who received platinum-based CT, with 2 patients having also undergone radiotherapy. The CIT cohort consisted of 8 patients (26.7%) who received immunotherapy (PD-1/PD-L1 inhibitors) combined with CT.

No significant differences were observed between the two treatment groups with regard to age, sex, smoking burden, histologic subtype, clinical stage, baseline tumor size, PD-L1 expression level or mutational status ($P>0.05$). However, given the limited sample size, group comparability should be interpreted with caution (Table I).

Tumor response and pathologic regression. When the primary endpoints of pathologic response were evaluated, a trend toward improved pathologic response was observed in the CIT cohort. The proportion of viable tumor cells in the resected specimens after treatment decreased to a median of 7.5% (IQR: 0.0-55.0) in the CIT group, whereas it remained at 55.0% (IQR: 32.5-67.5) in the CT group ($P=0.156$; Table II). Furthermore, mPR (≤10% viable tumor)

Table I. Clinical and pathological characteristics of patients according to treatment regimen.

Variable	Overall (n=30)	CIT (n=8)	CT (n=22)	P-value
Age, median years (IQR)	65.0 (59.2-68.5)	65.0 (55.5-71.5)	65.0 (62.2-67.0)	0.906
Sex (%)				0.064
Male	28 (93.3)	6 (75.0)	22 (100.0)	
Female	2 (6.7)	2 (25.0)	0 (0.0)	
Smoking history, median pack-years (IQR)	47.5 (22.5-60.0)	45.0 (11.2-65.0)	47.5 (30.0-60.0)	0.706
Histology, n (%)				0.215
Adenocarcinoma	15 (50.0)	6 (75.0)	9 (40.9)	
Squamous cell carcinoma	15 (50.0)	2 (25.0)	13 (59.1)	
Indication for neoadjuvant therapy, n (%)				0.369
Nodal involvement	16 (53.3)	6 (75.0)	10 (45.5)	
T4 disease/other	14 (46.7)	2 (25.0)	12 (54.5)	
Clinical stage, n (%)				0.789
IB-IIB	4 (13.3)	1 (12.5)	3 (13.6)	
IIIA	16 (53.3)	5 (62.5)	11 (50.0)	
IIIB-IVA	10 (33.3)	2 (25.0)	8 (36.4)	
Baseline tumor size, median cm (IQR)	5.7 (4.8-7.0)	5.3 (4.9-5.8)	5.9 (4.6-7.1)	0.439
PD-L1 expression, n (%)				0.340
Negative (<1%)	18 (60.0)	4 (50.0)	14 (63.6)	
Positive (≥1%)	12 (40.0)	4 (50.0)	8 (36.4)	
Mutation status, n (%)				0.284
Wild type (negative)	26 (86.7)	6 (75.0)	20 (90.9)	
Mutant	4 (13.3)	2 (25.0)	2 (9.1)	

CIT, chemo-immunotherapy; CT, chemotherapy; IQR, interquartile range; PD-L1, programmed death-ligand 1.

Table II. Post-treatment pathological findings and tumor microenvironment.

Morphologic feature	Overall (n=30)	CIT (n=8)	CT (n=22)	P-value
Postoperative tumor size, median cm (IQR)	2.8 (0.8-4.3)	1.6 (0.0-3.4)	2.9 (1.6-4.5)	0.268
Viable tumor, median % (IQR)	50.0 (10.0-67.5)	7.5 (0.0-55.0)	55.0 (32.5-67.5)	0.156
Tumor fibrosis, median % (IQR)	20.0 (12.5-30.0)	27.5 (20.0-42.5)	20.0 (10.0-30.0)	0.178
Tumor inflammation, median % (IQR)	15.0 (6.2-33.8)	32.5 (12.5-40.0)	10.0 (6.2-27.5)	0.274
Median tumor necrosis, % (IQR)	10.0 (5.0-20.0)	5.0 (4.5-21.2)	10.0 (5.0-18.8)	0.794
Total stroma, median % (IQR)	40.0 (20.5-68.8)	67.5 (39.2-91.2)	32.5 (20.0-57.5)	0.121
TIL pattern (lymphocytic), n (%)	12 (40.0)	5 (62.5)	7 (31.8)	0.210
pCR, n (%)	6 (20.0)	3 (37.5)	3 (13.6)	0.300
mPR, n (%)	10 (33.3)	5 (62.5)	5 (22.7)	0.078

CIT, chemo-immunotherapy; CT, chemotherapy; IQR, interquartile range; TIL, tumor-infiltrating lymphocyte; pCR, pathologic complete response; mPR, major pathologic response.

was achieved in 62.5% (5/8) of patients in the CIT cohort, compared with 22.7% (5/22) in the CT cohort. Statistical analysis showed that this difference approached significance (P=0.078; Table II). pCR (stage ypT0N0) was observed in 37.5% (3/8) of patients in the CIT group and 13.6% (3/22) of those in the CT group.

The depth of pathologic response in each patient is visualized in the waterfall plot (Fig. 3). Notably, patients receiving chemo-immunotherapy tended to cluster in the region associated with the greatest tumor regression, including pCR and mPR.

Tumor microenvironment and histologic changes. Histopathologic alterations occurring within the tumor bed in treatment-responsive patients, including fibrosis, inflammation, necrosis and stromal reactions, were analyzed (Table II). The total stromal component (fibrosis + inflammation)

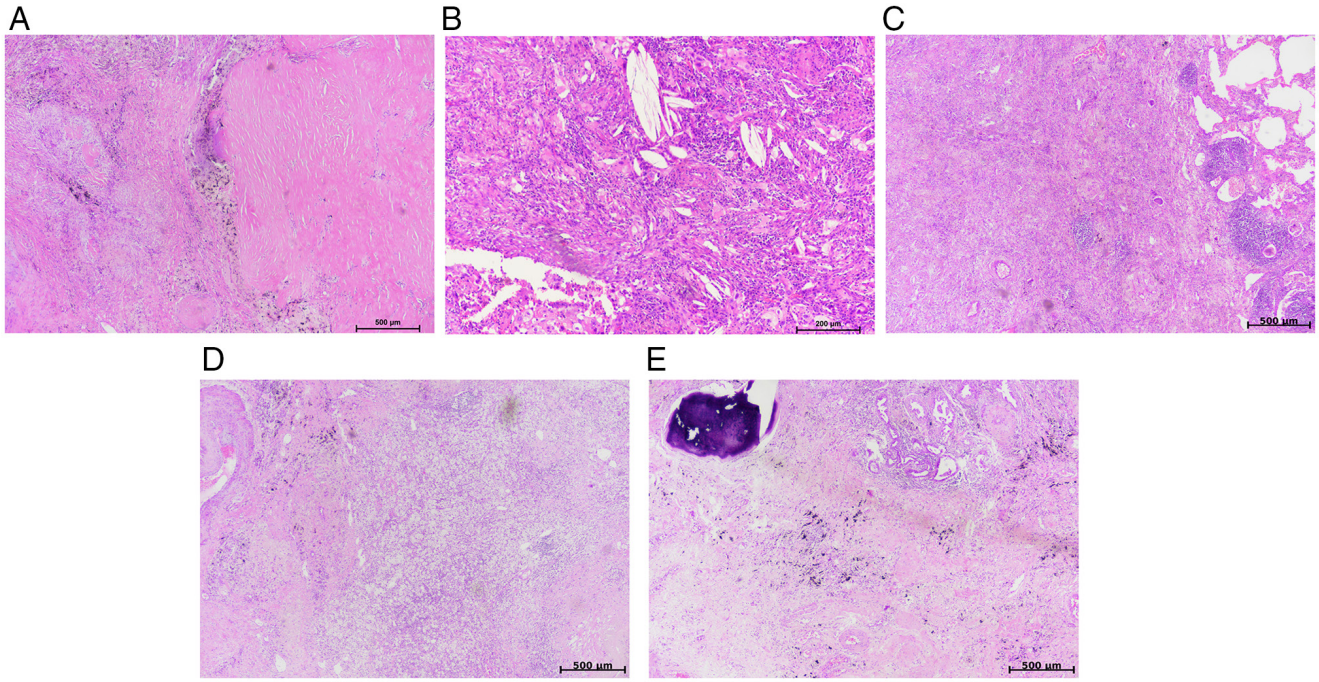

Figure 4. Major pathological response in the tumor bed. (A) Dense fibrosis and chronic inflammatory infiltrates (magnification x4). (B) Cholesterol clefts within the regressed tumor bed (H&E staining; original magnification x10). (C) Foreign body-type giant cell reaction (H&E staining; original magnification x4). (D) Prominent histiocytic accumulation (H&E staining; original magnification x4). (E) Microcalcifications within the fibrotic stroma (H&E staining; original magnification x4).

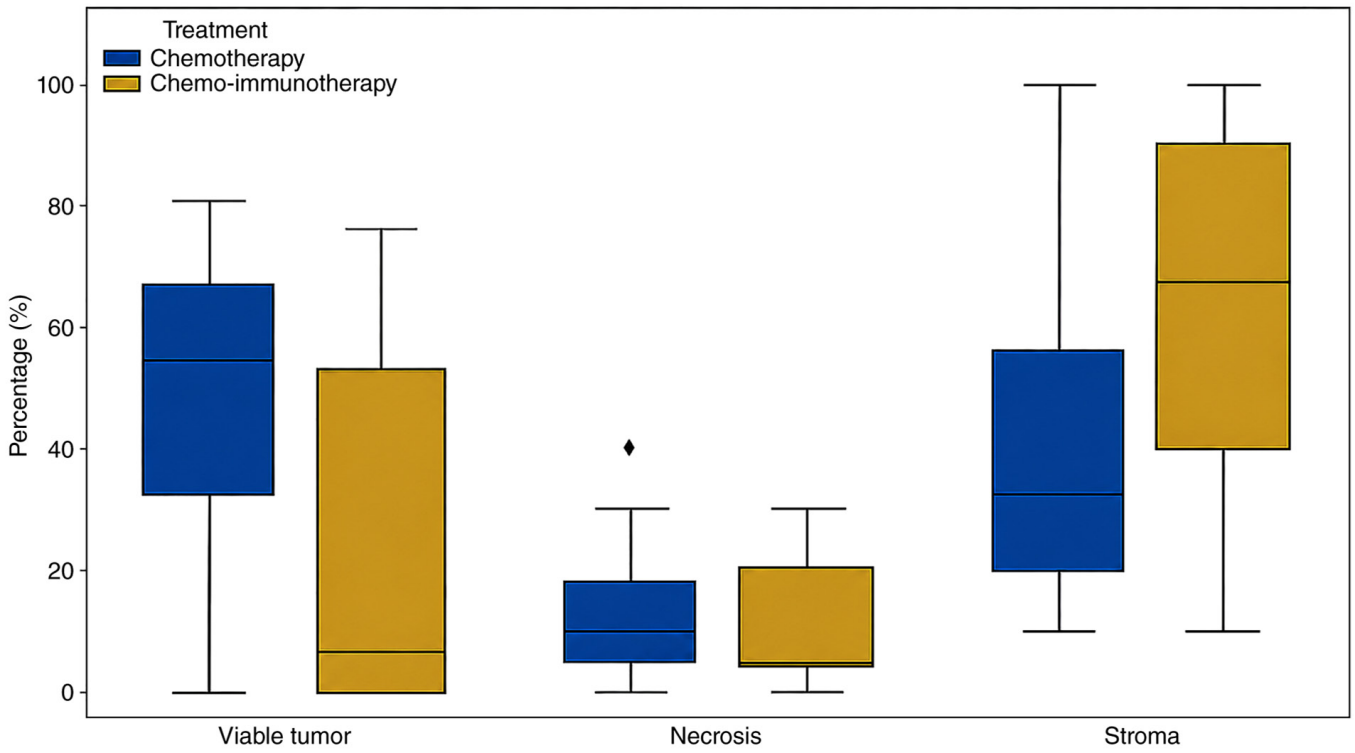

Figure 5. Distribution of viable tumor percentage, necrosis, and stromal components in the chemotherapy and chemo-immunotherapy groups after neoadjuvant treatment. The central line indicates the median, the box represents the interquartile range, and whiskers denote the minimum and maximum values. Outliers are indicated by black diamond symbol.

exhibited a median of 67.5% in the CIT group and 32.5% in the CT group. This suggested that immunotherapy not only promoted tumor regression but may have also promoted immune-mediated stromal remodeling within the tumor bed (Fig. 4A-E). Tumor-associated inflammation was found to be higher in the CIT cohort (median 32.5%) compared with

Table III. Spearman correlation analysis between PD-L1 expression and histopathologic variables.

Variable	PD-L1	Viable tumor	Necrosis	Fibrosis
PD-L1 score	1.00			
Viable tumor (%)	-0.17	1.00		
Necrosis (%)	-0.15	-0.09	1.00	
Fibrosis (%)	-0.06	-0.52[a]	0.08	1.00

[a]P<0.01. PD-L1, programmed cell death-ligand 1.

the CT cohort (10.0%). In addition, when TIL patterns were evaluated, a lymphocytic-dominant pattern was observed more frequently in the CIT group (62.5%) compared with the CT group (31.8%; Table II). Necrosis rates appeared to be similar between the two groups, indicating that necrosis did not serve as a distinguishing parameter of treatment response (P=0.794; Table II). These morphological changes are illustrated in the boxplot (Fig. 5), in which the viable tumor box lies markedly closer to the baseline in the CIT group, whereas the stromal component is shifted upward.

PD-L1-associated parameters. Correlation analysis revealed no significant associations between PD-L1 expression score and viable tumor percentage (rs=-0.17), necrosis (rs=-0.15), or fibrosis (rs=-0.06; P>0.05). A significant inverse correlation was observed between viable tumor percentage and fibrosis (rs=-0.52; P<0.01; Table III). The association between PD-L1 expression and the pattern of TILs (histiocytic vs. lymphocytic) was borderline significant (χ^2=5.92; P=0.052; Table III). Lymphocytic immune response was more pronounced in PD-L1-positive cases.

Treatment, clinical factors and response association. Results indicated that mPR was 62.5% in patients who received CIT, whereas it was 22.7% in the CT group (P=0.078; Table IV). The rate of pCR was found to be 37.5% in the CIT group and 13.6% in the CT group (P=0.300; Table II). Tumor shrinkage was found to be significantly greater in patients who achieved a pathologic response (pCR and mPR) compared with nonresponders (P<0.001 for both pCR and mPR; Table IV). No statistically significant association was found between pathologic response (pCR or mPR) and baseline clinical stage (P>0.05) or smoking burden (P>0.05).

Association between pathologic response (mPR and pCR) and tumor tissue characteristics/Histopathologic features of the tumor bed, including viable tumor, necrosis and fibrosis, were compared between responders (mPR/pCR) and nonresponders using the Mann-Whitney U test.

Both mPR and pCR responders exhibited significantly lower viable tumor percentages compared with nonresponders (P<0.001; Table V). Fibrosis, a strong indicator of treatment response, was found to be significantly higher in the mPR group (median: 40%) compared with the nonresponders (median: 20%; P<0.001; Table V). Similarly, fibrosis was significantly elevated in the pCR group (P=0.009; Table V), while tumor necrosis did not differ significantly between mPR and non-mPR groups or pCR and non-pCR groups (P=0.448 and P>0.99, respectively; Table V). STAS positivity was significantly lower in patients with mPR, indicating an inverse association (P<0.001). Despite pleural invasion being absent in patients with pCR, this finding was not statistically significant and therefore only reflected a trend (P>0.05; Table V).

PD-L1 and immune response. Comparisons between PD-L1-negative and PD-L1-positive groups revealed no significant differences in viable tumor percentage (P=0.305), necrosis (P=0.606) or fibrosis (P=0.761), and no significant association with achievement of mPR (P=0.693; Table VI). However, a lymphocytic TIL pattern was observed significantly more frequently in PD-L1-positive patients compared with PD-L1-negative patients (66.7% vs. 22.2%; P=0.040; Table VI).

Survival analysis. Given that the dataset lacked precise dates of mortality and recurrence, survival analysis was performed using a pseudo-OS approach, defined as the interval between diagnosis and the most recent follow-up. Within this framework, mPR was found to be associated with improved survival in the log-rank analysis (P=0.036). Increasing clinical stage was associated with higher mortality risk in the Cox regression model (HR=2.62; P=0.033). Higher tumor inflammation levels were also associated with improved survival (log-rank P=0.043), whereas tumor fibrosis and necrosis were not significantly associated with survival outcomes (P>0.05; data not shown).

Discussion

Neoadjuvant therapy is increasingly being used across numerous solid tumor types with the aim of reducing tumor burden and improving surgical resectability (6,10-12). This approach has been well established in malignancies such as breast, gastric and rectal cancer. The application of neoadjuvant therapy in NSCLC has gained increasing attention (2,3,13). One of the major challenges in NSCLC is that a marked proportion of patients may not proceed to surgical resection following neoadjuvant treatment because of disease progression or loss of operability. Consequently, the development of more effective neoadjuvant treatment strategies remains a necessity in this setting.

In this context, immunotherapy has emerged as a promising addition to conventional treatment approaches. As in other tumor types, accurate evaluation of post-treatment specimens is key, as characterization of the tumor bed provides important prognostic information. Histopathologic assessment serves a central role in this process. Therefore, understanding the histomorphological effects of CIT, beyond conventional CT-induced changes, is central to improving response assessment and guiding clinical decision-making in NSCLC.

In the present study, detailed assessment of pathologic response in resected NSCLC specimens following neoadjuvant therapy suggested that CIT may be associated with a more pronounced pattern of tumor regression compared with CT alone. Although these findings did not reach statistical significance, the lower proportion of RVT and the higher rates of mPR and pCR observed in the CIT group suggested a potential biological advantage of incorporating immunotherapy into neoadjuvant treatment. These findings

Table IV. Associations between clinical and treatment characteristics and mPR.

Variable	mPR present (n=10)	mPR absent (n=20)	P-value
Treatment regimen, n (%)			0.078
CIT	5 (62.5)	3 (37.5)	
CT	5 (22.7)	17 (77.3)	
Clinical stage, n (%)			0.449
I-II	1 (10.0)	3 (15.0)	
III-IV	9 (90.0)	17 (85.0)	
Smoking history, median pack-years (IQR)	57.5 (36-84)	43.5 (19-60)	0.508
Tumor size, median % (IQR)	-100.0 (-100 to -91)	-30.3 (-49 to -13)	<0.001

CIT, chemo-immunotherapy; CT, chemotherapy; mPR, major pathologic response; IQR, interquartile range.

Table V. Comparison of tumor tissue characteristics according to pathologic response status.

Variable	mPR present	mPR absent	P-value	pCR present	pCR absent	P-value
Viable tumor, median % (IQR)	0.0 (0.0-5.0)	60.0 (50.0-70.0)	<0.001	0.0 (0.0-0.0)	60.0 (40.0-70.0)	<0.001
Tumor fibrosis, median % (IQR)	40.0 (30.0-53.0)	20.0 (10.0-28.0)	<0.001	37.5 (31.0-55.0)	20.0 (10.0-30.0)	0.009
Tumor necrosis, median % (IQR)	10.0 (5.0-14.0)	7.5 (5.0-23.0)	0.448	7.5 (4.0-24.0)	10.0 (5.0-20.0)	0.990
STAS positivity (%)	20.0	70.0	0.012	0.0	66.7	<0.001
Pleural invasion (%)	0.0	30.0	0.061	0.0	25.0	0.191

mPR, major pathologic response; pCR, pathologic complete response; IQR, interquartile range; STAS, spread through air spaces.

Table VI. Comparison of histopathologic and clinical characteristics according to PD-L1 status.

Variable	PD-L1 negative (n=18)	PD-L1 positive (n=12)	Test	P-value
Viable tumor, median (%)	55.0	40.0	Mann-Whitney U	0.305
Tumor necrosis, median (%)	10.0	5.0	Mann-Whitney U	0.606
Tumor fibrosis, median (%)	20.0	20.0	Mann-Whitney U	0.761
mPR present, n (%)	5 (27.8)	5 (41.7)	χ^2	0.693
TIL pattern (lymphocytic), n (%)	4 (22.2)	8 (66.7)	χ^2	0.040

mPR, major pathologic response; PD-L1, programmed cell death-ligand 1; TIL, tumor-infiltrating lymphocytes.

should be interpreted as hypothesis-generating and are consistent with the explanatory framework provided by the IASLC recommendations, which emphasize standardized assessment of tumor bed composition and viable tumor quantification (5).

The regression patterns observed in the present cohort, including increased fibrosis and lymphocytic infiltration, broadly align with the immune-mediated changes described in the irPRC proposed by Cottrell *et al* (6). While these features are more frequently observed in immunotherapy-treated tumors, they should be interpreted within the context of treatment-related stromal remodeling. Increased TIL density may reflect a metabolically permissive tumor microenvironment, as tumor-derived factors (such as lactate) have been shown to suppress T cell function (9).

CheckMate 816 reported higher rates of mPR and pCR with the addition of immunotherapy to CT, supporting the potential contribution of immune activation to tumor regression (13). Similarly, the LCMC3 trial demonstrated that single-agent immunotherapy can induce measurable pathologic responses in early-stage NSCLC (14). However, given the limited sample size and lack of statistical significance in the present cohort, these observations should be interpreted cautiously.

Assessment of pathologic response in NSCLC resection specimens after neoadjuvant therapy presents notable challenges, particularly in distinguishing viable tumor from therapy-induced stromal changes and in accurately defining the boundaries of the tumor bed. The pathologist serves a critical role in the accurate assessment of

treatment response following neoadjuvant therapy, particularly through standardized evaluation and appropriate interpretation of post-treatment histologic changes (15). Weissferdt *et al* further demonstrated that appropriate sampling strategies, tumor bed mapping and recognition of immune-mediated regression features are central to accurate interpretation (16).

The differences observed between CIT and CT in the present study, namely greater fibrosis, a more pronounced inflammatory response, predominant lymphocytic TIL patterns and reduced STAS positivity, are broadly consistent with findings reported in the literature (17).

In a cohort study including 358 patients, Pataer *et al* (21) demonstrated that fibrosis is a reliable indicator of tumor response following neoadjuvant therapy (consistent with the present findings), whereas necrosis did not show a significant association with treatment response and lacks specificity as a marker of therapy-induced tumor regression. These patterns may reflect the combined effects of direct tumor cell death and immune-mediated remodeling of the tumor microenvironment. STAS has been recognized as an adverse prognostic factor associated with increased recurrence risk and aggressive tumor behavior in lung cancer (22). The reduced STAS positivity observed in mPR cases in the present study may reflect more effective elimination of invasive tumor components following neoadjuvant therapy. Assessment of STAS in post-neoadjuvant specimens may be challenging due to treatment-related architectural distortion and potential artifacts, which should be considered when interpreting its presence or absence.

Increased lymphocytic infiltration and stromal activation may represent an active immune response induced by immunotherapy. However, certain features should be interpreted with caution. Although increased fibrosis is frequently observed in responding tumors, it may partly reflect treatment-related tissue replacement rather than an independent predictive biomarker. Similarly, the assessment of STAS following neoadjuvant therapy may be influenced by treatment-induced architectural distortion and sampling variability. Therefore, these findings should be considered within the context of treatment effects and interpreted as descriptive rather than definitive indicators of tumor biology.

In the present study, nodal regression could not be adequately assessed, as there is currently no standardized method for the evaluation of post-neoadjuvant lymph node changes. In addition, lymph node assessment is challenging due to the frequent absence of distinct fibrotic regression patterns, with nodes often reverting to a near-normal appearance, and the presence of anthracosis and histiocytic aggregates that may further obscure treatment-related changes. Previous studies have shown that pathologic responses of the primary tumor and lymph nodes may frequently differ in NSCLC following neoadjuvant CIT (23,24). Joint evaluation of both primary tumor and nodal responses is important in accurate prognostic stratification and the lack of comprehensive assessment of nodal regression represents one of the limitations of the present study (25). The association between TIL enrichment and pathologic response in the present cohort also aligns with biomarker-focused studies such as that of Rojas *et al* (26).

In the present study, pathologic evaluation was performed jointly by three pathologists. In a study addressing the subjectivity of mPR assessment in NSCLC after neoadjuvant therapy, interobserver agreement among pathologists was found to be high; in addition, the ≤10% viable tumor threshold was shown to be a reliable criterion for predicting survival. Therefore, standardized assessment is of marked importance in clinical research and patient management (27).

It should be noted that certain associations observed in the present study may be partly influenced by the definitions of response criteria. For example, the lower viable tumor percentage in mPR cases is inherent to the definition of mPR rather than an independent biological finding. In addition, given the relatively small sample size and the number of subgroup analyses performed, a number of the observed associations should be interpreted as exploratory. Future studies with larger cohorts and validation analyses are thus required to further determine these findings.

Due to the absence of precise data regarding recurrence and mortality, survival outcomes in the present study were assessed using a pseudo-OS metric, which does exhibit inherent limitations. Within this exploratory framework, mPR appeared to be associated with improved survival, consistent with previous studies reporting an association between RVT and clinical outcomes (7,16,21). Similarly, increased tumor-associated inflammation exhibited a trend toward improved survival. Meta-analytic data have suggested that CIT may improve survival outcomes and increase pCR rates in NSCLC (28). However, these observations should be interpreted cautiously, as pseudo-OS may be influenced by follow-up duration, censoring patterns and treatment-associated factors, such as differences in neoadjuvant regimens, variability in treatment response and the use of adjuvant therapy. Therefore, these findings should be considered hypothesis-generating rather than definitive evidence of prognostic importance. Previous studies have suggested that the degree of histologic tumor regression after neoadjuvant therapy in NSCLC may serve as a potential biomarker for predicting patient survival (7,21,29).

In routine practice, assessment of pathologic response provides an early indication of treatment effectiveness and may help guide clinical decision-making. In the context of neoadjuvant or perioperative CIT, standardized pathologic evaluation remains particularly important for both patient management and research (30).

In the present study, a higher degree of tumor inflammation and increased TIL density were observed following CIT. However, a number of studies have reported that, although immunotherapy is associated with greater lymphocytic infiltration and more prominent immune response features within the tumor microenvironment, the overall patterns of pathological regression, including fibrosis, necrosis and residual viable tumor distribution, largely overlap with those seen after CT (6,17,26,30). The degree of pathologic response, particularly mPR and pCR, is a strong predictor of survival in patients treated with both immunotherapy and CT (31). These findings further suggest an important role for the tumor microenvironment in shaping treatment response.

Despite this, the applicability of a uniform ≤10% viable tumor threshold across all histologic subtypes has been questioned.

Qu *et al* (32) demonstrated that the optimal cut-off for RVT differs markedly between adenocarcinoma and squamous cell carcinoma when these tumor types are evaluated separately and that a higher threshold is required for prognostic stratification in adenocarcinomas; however, in the present study, adenocarcinoma and squamous cell carcinoma were not analyzed separately and were instead evaluated categorically under the umbrella of NSCLC. In this context, although the ≤10% cut-off was applied in accordance with guidelines (5), it is conceivable that histology-specific cut-off values may be adopted in future studies. This further supports the need for subtype-specific interpretation of pathologic response in NSCLC.

Despite the promising efficacy of immunotherapy, a notable proportion of patients with NSCLC develop either primary or acquired resistance to treatment. As highlighted by Wang *et al* (33), immunotherapy resistance is a multifactorial process involving tumor-intrinsic genetic alterations, dysregulation of immune checkpoint pathways and the establishment of an immunosuppressive tumor microenvironment. These mechanisms may impair effective T-cell activation, reduce immune cell infiltration and ultimately limit treatment response. In this context, the tumor microenvironment emerges as a key determinant of therapeutic efficacy, aligning with the present findings demonstrating associations between inflammatory response and treatment-associated changes. Notably, the development of resistance underscores the need for alternative and combinatorial treatment strategies, including the integration of targeted therapies, anti-angiogenic agents and novel immunomodulatory approaches. This is particularly relevant to the present findings, in which variations in inflammatory response and TIL density may reflect underlying differences in tumor immune competence and potential resistance mechanisms. These observations may have implications for treatment stratification and response assessment in the neoadjuvant setting, particularly in distinguishing effective immune-mediated responses from residual disease.

Emerging therapeutic strategies, including macrophage-mediated nanomedicine delivery systems and nano-assisted radiotherapy approaches, further highlight the active role of the tumor microenvironment in modulating therapeutic response in lung cancer (34,35).

An additional consideration is the potential confounding effect of radiotherapy, as a subset of patients in the CT cohort also received radiotherapy. Radiotherapy is known to influence tumor morphology by increasing necrosis, promoting fibrosis and altering stromal composition, which may complicate the distinction between viable tumor and treatment-related changes and thereby affect histopathological assessment (29,36). However, only a limited number of patients (n=2) received combined chemoradiotherapy in the present cohort. Upon evaluation of these cases, both demonstrated minimal pathologic response, suggesting that radiotherapy is unlikely to have contributed markedly to the regression patterns observed in the present cohort. Although radiotherapy may induce prominent histopathologic alterations such as fibrosis and tissue remodeling, these changes do not necessarily reflect a strong therapeutic response and may complicate the distinction between viable tumor and treatment effect, as previously reported in radiotherapy-treated NSCLC resection specimens (36). This factor should be considered when interpreting the results. Given that only a small number of patients received radiotherapy, subgroup analysis was not feasible (36).

Pathologic complete response is considered an important parameter in the assessment of patient prognosis; however, it is not always sufficient as a standalone indicator. As highlighted by Huynh *et al* (37), long-term survival is influenced not only by the extent of tumor eradication but also by tumor biology, treatment modality and characteristics of the tumor microenvironment such as TIL density, patterns of immune response, and stromal composition including fibrosis and inflammatory cell infiltration. Therefore, even in cases without pathologic complete response, prognostic evaluation should not rely solely on the presence of residual tumor but should also incorporate a comprehensive assessment of the tumor microenvironment and immune response. This perspective is consistent with the present findings, in which variations in inflammatory response and TIL density were associated with treatment-associated changes.

Recent advances in artificial intelligence (AI)-assisted pathology have further emphasized the value of objective response assessment. In the LCMC3 study, Dacic *et al* (38) demonstrated that AI-powered quantification of pathologic response in NSCLC treated with neoadjuvant atezolizumab provides reproducible and scalable evaluation of tumor regression. These findings support the integration of digital pathology tools, such as QuPath, into routine practice to enhance the accuracy and consistency of post-treatment assessment.

Collectively, the present findings suggest that CIT may be associated with a more pronounced pattern of pathologic response compared with CT alone. These observations are consistent with the growing body of evidence supporting the role of neoadjuvant immunotherapy in resectable NSCLC and thus emphasize the importance of standardized pathologic response assessment in both clinical practice and research settings (4,13,14). These findings also highlight the evolving role of the tumor microenvironment as a key determinant of treatment response.

The present study is limited by its relatively small sample size and single-center, retrospective design, which may introduce selection bias and restrict generalizability. The limited number of cases reflects the restricted availability of resected specimens following neoadjuvant therapy in routine clinical practice, as not all patients proceed to surgery after systemic treatment. In addition, treatment heterogeneity across patients may have influenced the observed patterns of pathologic response and the absence of precise recurrence and mortality data limited the ability to conduct conventional survival analyses. In addition, the use of pseudo-OS may have introduced bias related to variability in follow-up duration and censoring patterns and the limited number of survival events further restricts the strength and interpretability of survival-associated findings. Furthermore, the inclusion of a small number of patients who received radiotherapy in addition to CT may have influenced histopathologic features such as necrosis, fibrosis and stromal remodeling. Although evaluation of these cases demonstrated minimal pathologic response, the potential confounding effect of radiotherapy cannot be entirely excluded and should be interpreted with caution.

Additional limitations may have included the lack of formal interobserver agreement analysis. Although all cases were evaluated jointly by three pathologists using a

consensus-based approach, some variability in the assessment of histologic parameters such as fibrosis, inflammation and viable tumor cannot be entirely excluded. Furthermore, the absence of blinding to treatment groups may have introduced potential bias. Lastly, given that manual annotation was required for region selection, a degree of observer-dependent variability remains unavoidable, despite digital image analysis using QuPath having provided a more objective and reproducible framework for quantifying tumor, stromal and necrotic components.

In conclusion, neoadjuvant CIT may be associated with deeper pathologic regression compared with CT alone, characterized by increased fibrosis and enhanced immune activation, including higher TIL density and reduced STAS positivity. In addition, mPR may serve as a potential prognostic indicator. Overall, integration of IASLC and irPRC criteria, together with tumor microenvironment assessment, may improve the evaluation of treatment response in resectable NSCLC.

Acknowledgements

Not applicable.

Funding

No funding was received.

Availability of data and materials

The data generated in the present study may be requested from the corresponding author.

Authors' contributions

ÖKK conceived and designed the study, performed histopathological evaluation and wrote the manuscript. YSÇ and NSB performed histopathological evaluation and interpreted clinicopathological data. MB performed statistical analysis and assisted with retrieving and organizing patient data from the hospital information system. All authors have read and approved the manuscript. ÖKK and MB confirm the authenticity of all the raw data.

Ethics approval and consent to participate

The present study was conducted in accordance with the Declaration of Helsinki and was approved by the Institutional Ethics Committee of Etlik City Hospital (Ankara, Turkey; approval no: AEŞH-BADEK2-2025-285). Due to the retrospective nature of the present study, the requirement for informed consent was waived by the ethics committee.

Patient consent for publication

Not applicable.

Competing interests

The authors declare that they have no competing interests.

References

1. Thai AA, Solomon BJ, Sequist LV, Gainor JF and Heist RS: Lung cancer. Lancet 398: 535-554, 2021.
2. Provencio M, Nadal E, Insa A, García-Campelo MR, Casal-Rubio J, Dómine M, Majem M, Rodríguez-Abreu D, Martínez-Martí A, De Castro Carpeño J, *et al*: Neoadjuvant chemotherapy and nivolumab in resectable non-small-cell lung cancer (NADIM): An open-label, multicentre, single-arm, phase 2 trial. Lancet Oncol 21: 1413-1422, 2020.
3. Wakelee H, Liberman M, Kato T, Tsuboi M, Lee SH, Gao S, Chen KN, Dooms C, Majem M, Eigendorff E, *et al*: Perioperative pembrolizumab for early-stage non-small-cell lung cancer. N Engl J Med 389: 491-503, 2023.
4. Sorin M, Prosty C, Ghaleb L, Nie K, Katergi K, Shahzad MH, Dubé LR, Atallah A, Swaby A, Dankner M, *et al*: Neoadjuvant chemoimmunotherapy for NSCLC: A systematic review and meta-analysis. JAMA Oncol 10: 621-633, 2024.
5. Travis WD, Dacic S, Wistuba I, Sholl L, Adusumilli P, Bubendorf L, Bunn P, Cascone T, Chaft J, Chen G, *et al*: IASLC multidisciplinary recommendations for pathologic assessment of lung cancer resection specimens after neoadjuvant therapy. J Thorac Oncol 15: 709-740, 2020.
6. Cottrell TR, Thompson ED, Forde PM, Stein JE, Duffield AS, Anagnostou V, Rekhtman N, Anders RA, Cuda JD, Illei PB, *et al*: Pathologic features of response to neoadjuvant anti-PD-1 in resected non-small-cell lung carcinoma: A proposal for quantitative immune-related pathologic response criteria (irPRC). Ann Oncol 29: 1853-1860, 2018.
7. Hou Z, Zhao L, Zou L and Li B: The prognostic value of tumor-infiltrating lymphocytes in non-small cell lung cancer patients who received neoadjuvant chemotherapy followed by surgery. Adv Clin Exp Med 32: 847-853, 2023.
8. Yan Q, Li S, He L and Chen N: Prognostic implications of tumor-infiltrating lymphocytes in non-small cell lung cancer: A systematic review and meta-analysis. Front Immunol 15: 1476365, 2024.
9. Fischer K, Hoffmann P, Voelkl S, Meidenbauer N, Ammer J, Edinger M, Gottfried E, Schwarz S, Rothe G, Hoves S, *et al*: Inhibitory effect of tumor cell-derived lactic acid on human T cells. Blood 109: 3812-3819, 2007.
10. Tetzlaff MT, Messina JL, Stein JE, Xu X, Amaria RN, Blank CU, van de Wiel BA, Ferguson PM, Rawson RV, Ross MI, *et al*: Pathological assessment of resection specimens after neoadjuvant therapy for metastatic melanoma. Ann Oncol 29: 1861-1868, 2018.
11. Rizzo A, Mollica V, Santoni M, Palmiotti G and Massari F: Pathologic complete response in urothelial carcinoma patients receiving neoadjuvant immune checkpoint inhibitors: A meta-analysis. J Clin Med 11: 1038, 2022.
12. Symmans WF, Peintinger F, Hatzis C, Rajan R, Kuerer H, Valero V, Assad L, Poniecka A, Hennessy B, Green M, *et al*: Measurement of residual breast cancer burden to predict survival after neoadjuvant chemotherapy. J Clin Oncol 25: 4414-4422, 2007.
13. Forde PM, Spicer J, Lu S, Provencio M, Mitsudomi T, Awad MM, Felip E, Broderick SR, Brahmer JR, Swanson SJ, *et al*: Neoadjuvant nivolumab plus chemotherapy in resectable lung cancer. N Engl J Med 386: 1973-1985, 2022.
14. Chaft JE, Oezkan F, Kris MG, Bunn PA, Wistuba II, Kwiatkowski DJ, Owen DH, Tang Y, Johnson BE, et al: Neoadjuvant atezolizumab for resectable non-small cell lung cancer: An open-label, single-arm phase II trial. Nat Med 28: 2155-2161, 2022..
15. Dacic S: Neoadjuvant therapy and lung cancer: Role of pathologists. Arch Pathol Lab Med 149: e78-e81, 2025.
16. Weissferdt A, Leung CH, Lin H, Sepesi B, William WN, Swisher SG, Cascone T, Lee JJ and Pataer A: Pathologic processing of lung cancer resection specimens after neoadjuvant therapy. Mod Pathol 37: 100353, 2024.
17. Alì G, Poma AM, Di Stefano I, Zirafa CC, Lenzini A, Martinelli G, Romano G, Chella A, Baldini E, Melfi F and Fontanini G: Different pathological response and histological features following neoadjuvant chemotherapy or chemo-immunotherapy in resected non-small cell lung cancer. Front Oncol 13: 1115156, 2023.
18. Liu Z, Gao Z, Zhang M, Wang X, Gong J, Jiang S and Zhang Z: Real-world effectiveness and prognostic factors analysis of stages I-III non-small cell lung cancer following neoadjuvant chemo-immunotherapy or neoadjuvant chemotherapy. Ann Thorac Cardiovasc Surg 28: 111-120, 2022.

19. Kalvapudi S, Vedire Y, Yendamuri S and Barbi J: Neoadjuvant therapy in non-small cell lung cancer: Basis, promise, and challenges. Front Oncol 13: 1286104, 2023.
20. Bankhead P, Loughrey MB, Fernández JA, Dombrowski Y, McArt DG, Dunne PD, McQuaid S, Gray RT, Murray LJ, Coleman HG, *et al*: QuPath: Open source software for digital pathology image analysis. Sci Rep 7: 16878, 2017.
21. Pataer A, Kalhor N, Correa AM, Raso MG, Erasmus JJ, Kim ES, Behrens C, Lee JJ, Roth JA, Stewart DJ, *et al*: Histopathologic response criteria predict survival of patients with resected lung cancer after neoadjuvant chemotherapy. J Thorac Oncol 7: 825-832, 2012.
22. Kadota K, Nitadori JI, Sima CS, Ujiie H, Rizk NP, Jones DR, Adusumilli PS and Travis WD: Tumor spread through air spaces is an important pattern of invasion and impacts the frequency and location of recurrences after limited resection for small stage I lung adenocarcinomas. J Thorac Oncol 10: 806-814, 2015.
23. Ma R, Yang H, Ge Y, Ma T, Wang J, Li S, Feng T, Feng S, Zhang C, Sun T, *et al*: Prognostic implications of lymph node status in non-small-cell lung cancer patients before and after neoadjuvant chemoimmunotherapy: A multicenter retrospective study. Clin Lung Cancer 26: 370-383, 2025.
24. Chiappetta M, Tabacco D, Iaffaldano AG, Evangelista J, Congedo MT, Sassorossi C, Meacci E, D'Argento E, Bria E, Vita E, *et al*: Clinical stage III NSCLC patients treated with neoadjuvant therapy and surgery: The prognostic role of nodal characteristics. Life (Basel) 12: 1753, 2022.
25. Huang S, Wu J, Li S, Li X, Zeng R, Tang Y, Tang J, Ben X, Zhang D, Xie L, *et al*: Evaluation of combined pathological responses in primary tumor and lymph nodes following neoadjuvant chemoimmunotherapy in non-small cell lung cancer. Lung Cancer 186: 107401, 2023.
26. Rojas F, Parra ER, Wistuba II, Haymaker C and Solis Soto LM: Pathologic response and immune biomarker assessment in non-small-cell lung carcinoma receiving neoadjuvant immune checkpoint inhibitors. Cancers (Basel) 14: 2775, 2022.
27. Kim S, Lee J and Chung JH: Histological assessment and interobserver agreement in major pathologic response for non-small cell lung cancer with neoadjuvant therapy. Cancer Res Treat 57: 401-411, 2025.
28. Banna GL, Hassan MA, Signori A, Giunta EF, Maniam A, Anpalakhan S, Acharige S, Ghose A and Addeo A: Neoadjuvant chemo-immunotherapy for early-stage non-small cell lung cancer: A systematic review and meta-analysis. JAMA Netw Open 7: e246837, 2024.
29. Junker K, Thomas M, Schulmann K, Klinke F, Bosse U and Müller KM: Tumour regression in non-small-cell lung cancer following neoadjuvant therapy. Histological assessment. J Cancer Res Clin Oncol 123: 469-477, 1997.
30. Elsner F, Kümpers C, Ott G, Döring J, Schildknecht K, Fisseler-Eckhoff A, von Laffert M, Baier L, Giulini L, Kraus D, *et al*: Current practice of pathologic response assessment following chemoimmunotherapy for non-small cell lung cancer (NSCLC) in Germany: First real-world data from the multicentre Re-GraDE study. Histopathology 87: 869-879, 2025.
31. Nie F, Wang Y, Shi W, Zhu L, Hao J and Tao R: Prognosis prediction using significant pathological response following neoadjuvant immunotherapy in resectable non-small-cell lung tumors: A meta-analysis. Front Surg 11: 1500593, 2024.
32. Qu Y, Emoto K, Eguchi T, Aly RG, Zheng H, Chaft JE, Tan KS, Jones DR, Kris MG, Adusumilli PS and Travis WD: Pathologic assessment after neoadjuvant chemotherapy for NSCLC: Importance and implications of distinguishing adenocarcinoma from squamous cell carcinoma. J Thorac Oncol 14: 482-493, 2019.
33. Wang H, Niu X, Jin Z, Zhang S, Fan R, Xiao H and Hu SS: Immunotherapy resistance in non-small cell lung cancer: From mechanisms to therapeutic opportunities. J Exp Clin Cancer Res 44: 250, 2025.
34. Liu C, Chen Y, Xu X, Yin M, Zhang H and Su W: Utilizing macrophages missile for sulfate-based nanomedicine delivery in lung cancer therapy. Research (Wash D C) 7: 0448, 2024.
35. Zhao L, Li M, Shen C, Luo Y, Hou X, Qi Y, Huang Z, Li W, Gao L, Wu M and Luo Y: Nano-assisted radiotherapy strategies: New opportunities for treatment of non-small cell lung cancer. Research (Wash D C) 7: 0429, 2024.
36. Roy SF, Louie AV, Liberman M, Wong P and Bahig H: Pathologic response after modern radiotherapy for non-small cell lung cancer. Transl Lung Cancer Res 8 (Suppl 2): S124-S134, 2019.
37. Huynh C, Sorin M, Rayes R, Fiset PO, Walsh LA and Spicer JD: Pathological complete response as a surrogate endpoint after neoadjuvant therapy for lung cancer. Lancet Oncol 22: 1056-1058, 2021.
38. Dacic S, Travis WD, Giltnane JM, Kos F, Abel J, Hilz S, Fujimoto J, Sholl L, Ritter J, Khalil F, *et al*: Artificial intelligence-powered assessment of pathologic response to neoadjuvant atezolizumab in patients with NSCLC: Results from the LCMC3 study. J Thorac Oncol 19: 719-731, 2024.